Supplementary Information

Fabian Bauch,[†] Chuan-Ding Dong,[*,†] and Stefan Schumacher[†]

†*Department of Physics and Center for Optoelectronics and Photonics Paderborn (CeOPP), Paderborn University, Warburger Strasse 100, 33098 Paderborn, Germany*

‡*Wyant College of Optical Sciences, University of Arizona, Tucson, AZ 85721, USA*

E-mail: cddong@mail.uni-paderborn.de

Computational methods

AIMD in brief: In ab initio molecular dynamics (AIMD) simulations the forces acting on the nuclei are computed from electronic structure calculations that are performed "on-the–fly" as the molecular dynamics trajectory is generated [1]. As noted in the ORCA manual [2], the AIMD simulation used in this work follows the scheme of Born-Oppenheimer molelcular dynamics, where the time-independent Schrödinger equation is solved to compute the potential energy gradient, and then move the atoms according to these gradients.

Berendsen thermostat in brief: In MD simulations in the canonical ensemble, a thermostat is introduced to scale the temperature of the system, or to exchange energy with the thermal bath, to ensure an average system temperature. Different approaches such as the Anderson thermostat, the Nosé-Hoover thermostat, the Gaussian thermostat, and the Berendsen thermostat can be used. The Berendsen thermostat [3] represents a weak coupling to the thermal bath, and allows fluctuations of the temperature. In the Berendson thermostat, at each time step of the MD simulation, the velocities are scaled to a rate proportional to the difference between the current temperature and the bath temperature, as to drive the system temperature towards the bath temperature.

[1] D. Marx and J. Hutter, Ab Initio Molecular Dynamics: Basic Theory and Advanced Methods, (Cambridge University Press, Cambridge 2009).

[2] Martin Brehm, ORCA 5.0 Molecular Dynamics Module, https://brehm-research.de/orcamd

[3] Berendsen, H. J. C.; Postma, J. P. M.; vanGunsteren, W. F.; DiNola, A.; Haak, J. R. J. Chem. Phys. 81(8), 3684 (1984).

Figure S1 illustrates the two different types of charge motion induced by vibrational modes, namely intrachain and interchain charge transfer, where the charge is represented by the β-LUMO. Normal mode 235 shows charge movement within a polymer chain (intrachain), which is a common behavior for this class of materials, while normal mode 258 shows charge transfer movement from one polymer chain to another polymer chain (interchain). Both motions are consistent with the charge composition of the polymer chains caused by mode stretching, as explained in the main text.
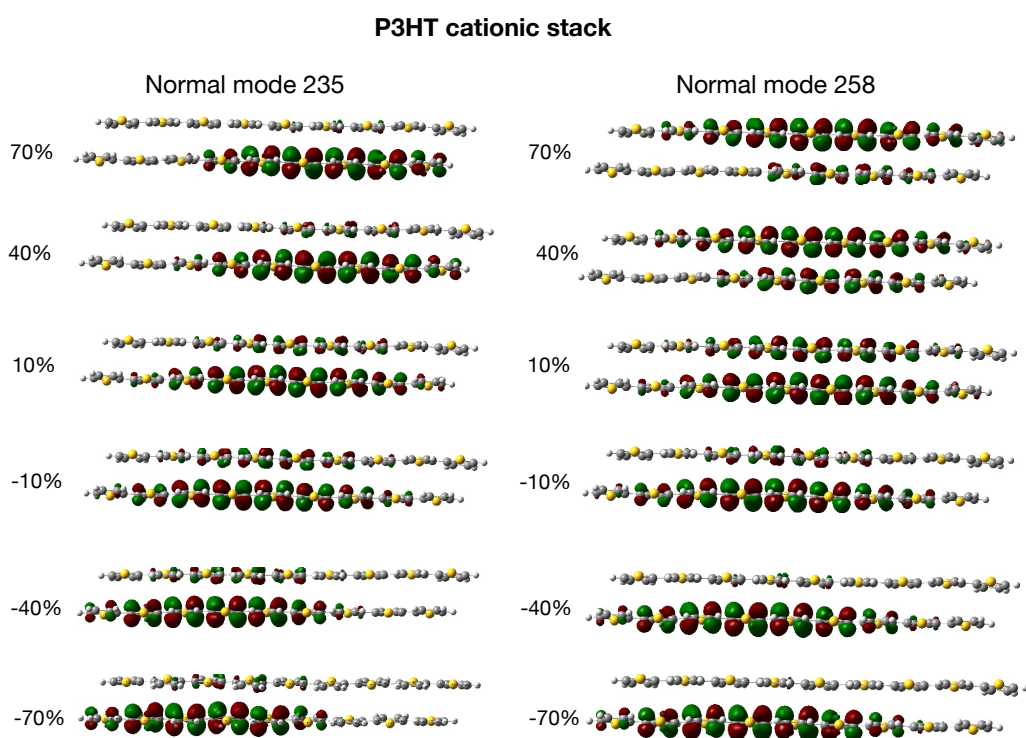
P3HT cationic stack

Figure S1: The intrachain and interchain motions of polaron in the calculated normal modes 235 and mode 258 in the cationic P3HT stack, shown by the orbitals at different percentage of stretching along the mode (labelled on the left side of each orbital figure). Mode 235 shows the intrachain motion, and mode 258 the interchain motion.

Figure S2 shows the analysis of vibrational modes for shorter polymer chains compared to the main text. Both interchain and intrachain charge transfer modes are observed for both materials, indicating a dependence of the mode characteristics on polymer length.

Two different characteristic classifications of these modes can be identified: i) charge transfer modes characterized by antisymmetric carbon-carbon stretching patterns of the same corresponding bonds of both polymers and strong charge transfer between the polymers upon displacement of atoms along these modes, and ii) non-charge transfer modes exhibiting symmetric bond stretching and negligible charge transfer upon displacement of atoms along these modes.
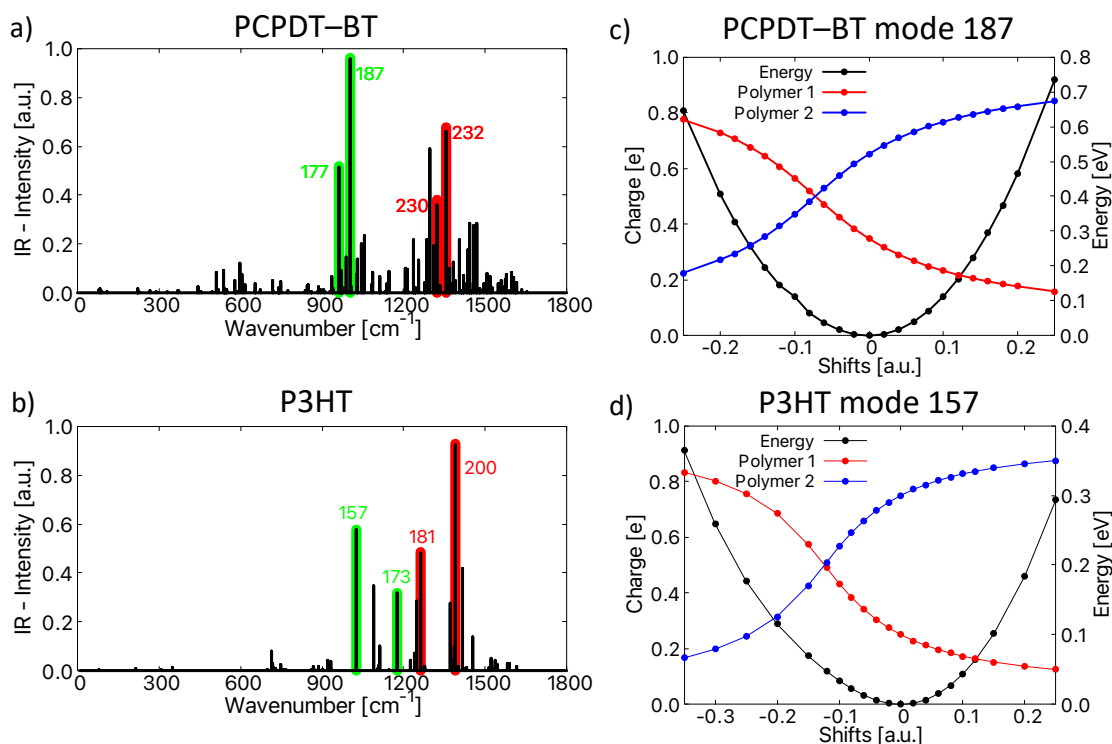

Figure S2: The interchain CT associated with the vibrational normal modes of PCPDTBT stack and P3HT stack with reduced sizes of oligomers. The PCPDTBT oligomer has 2 BT units and 2 CPDT units, while the P3HT oligomer has 6 repeat units. a) and b) show the calculated vibrational spectra, where several modes with relatively strong intensities are selected to address the interchain CT. The modes marked by green are found to facilitate interchain CT, and the ones marked by red are found without interchain CT. c) and d) show the energy change and the net charge on each oligomer for the mode 187 of PCPDTBT, and for the mode 157 of P3HT.

Figure S3 shows the evolution of the total energy and temperature in the molecular dynamics simulation of both materials. Here, the total energy is the energy of the electronic system from the static DFT part of the AIMD calculations, which includes kinetic energy, Hartree energy, exchange-correlation interaction, Coulomb attraction with nuclei, as well as Van der Waals interaction correction for all the electrons. Both quantities increase rapidly at first and then fluctuate around similar constant values, indicating that both temperature and energy are in equilibrium after about 100 fs. The charge transfer features explained in the main text do not occur qualitatively in either the energy or the temperature, so the charge transfer features appear to be a continuous process in equilibrium.
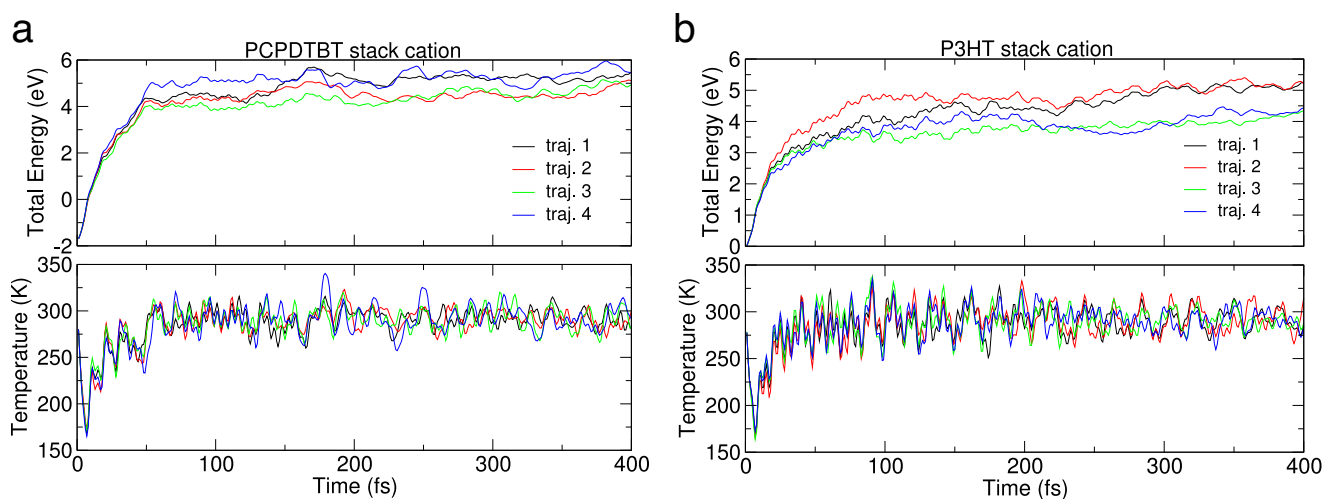

Figure S3: The evolution of total energies and temperatures of a) PCPDTBT cationic stack and b) P3HT cationic stack in the AIMD simulation. Four trajectories are given, corresponding to those shown in Figure 3 in the main text.